NOAA OPERATIONAL SOUNDING PRODUCTS FOR ADVANCED-TOVS

Anthony L. Reale
NOAA/NESDIS
Washington D.C.

INTRODUCTION

The National Oceanic and Atmospheric Administration, National Environmental Satellite Data and Information Service (NESDIS) operates a fleet of civilian, polar orbiting environmental satellites which provide users and researchers with a suite of atmospheric and surface measurements, and derived products on a global scale. On May 13, 1998, the Advanced TIROS Operational Vertical Sounder (ATOVS) radiometer configuration onboard NOAA-15 was successfully deployed into a morning orbit, replacing TOVS, followed by NOAA-16 into an afternoon orbit, on September 21, 2000, and NOAA-17 on June 22, 2002, which was launched into a mid morning orbit half way between NOAA-16 and NOAA-17. The ATOVS featured the Advanced Microwave Sounding Unit which replaced the MSU and SSU, along with the 20-channel HIRS/3 and a 6-channel Advanced Very High Resolution Radiometer (AVHRR/3) similar to its predecessors. The following report summarizes the processing systems for deriving the NESDIS operational ATOVS sounding products and provides a review of the derived weather products and evaluation results for the current 3-satellite configuration of ATOVS operational satellites.

ORBITAL PROCESSING

A brief summary of the scientific algorithms comprising the orbital processing system is provided, for further details see Reale (2001 and 2002).

The **Orbital** processing system provides:

- Pre-processing,
- Contamination detection,
- First guess and retrieval for soundings, and
- Cloud, Radiation, and Total Ozone products.

Pre-processing steps include instrument calibration, quality control (QC) of the sounder measurements, attachment of ancillary data such as terrain designation, Sea Surface Temperature, and numerical weather prediction (NWP) forecasts, the spatial interpolation of the AMSU-A measurements to the HIRS/3 fields-of-view, and measurement adjustment to the nadir view (Allegrino *et al.* 1999).

Contamination detection consists of the identification of effects due to precipitation on the AMSU measurements, and due to clouds for the HIRS/3 measurements. Global cloud detection (Ferguson and Reale 2000) and the resulting cloud-mask constrain the use of HIRS in subsequent retrieval steps.

The **first guess** is uniquely determined for each sounding using a library search technique (Goldberg *et al.* 1988). The libraries consist of segregated samples of collocated radiosonde and satellite measurements (Tilley *et al.* 2000) which are updated on a daily basis and which are directly accessed during orbital processing.

The first guess is obtained by minimizing an equation equivalent to (1):

$$D = (R - R_k)^t \, B^{-1} \, (R - R_k) \qquad (1)$$

where the superscript *t* indicates the matrix transpose, -1 the inverse, and

D : scalar closeness parameter,
B : sounding channel radiance covariance matrix; dimension (35 x 35),
R : adjusted, observed radiance temperature vector; dimension ($N_{A,i}$), and
R_k : adjusted, library radiance temperature vector; dimension ($N_{A,i}$).

The B-matrix is computed consistent with the collocation library searched for a given sounding, and is updated daily. The dimension "35" for the B matrix in denotes the total number of sounder channels available from ATOVS; not all are used. The dimension ($N_{A,i}$) denotes the specific channel combination used to compute D, and the subscript "k" denotes the collocations searched. The channel combination for a given sounding varies depending on whether the sounding type is clear or cloudy, and sea or non-sea. The actual first guess temperature, moisture and radiance temperature profiles for a given sounding are computed by averaging the 10 closest collocations with smallest D.

The **retrieval** is done using a Minimum Variance Simultaneous solution (Fleming *et al.* 1986), which is given by equation (2):

$$T - T_g = S A^t \, (A S A^t + N)^{-1} \, (R - R_g) \qquad (2)$$

where the subscript *t* indicates the matrix transpose, -1 the inverse, and:

T: final soundings products vector, (133),
T_g: first guess products vector, (133)
S: first guess covariance matrix, (133 x 133),
A: sounder channel weighting matrix, (35 x 133),
N: measurement uncertainty matrix, (35 x 35),
R: observed radiance temperature vector, ($M_{A,j}$), and
R_g : first guess radiance temperature vector, ($M_{A,j}$).

The internal product vector (T) includes one-hundred (100) levels of atmospheric temperature (1000mb to .1mb), thirty-two (32) levels of moisture (1000mb to 200mb), and the surface temperature. The dimension thirty-five (35) for the A and N matrices denotes the available ATOVS channels; not all are used. The dimension ($M_{A,j}$) denotes the specific channel combination used for retrieval depending on the sounding type.

The S, A and N matrices of Equation-2, along with the B-matrix of Equation-1 are computed based on the latest collocations of radiosonde and satellite data, and updated weekly (Tillet *et al.* 2000). There are four (4) separate B-matrices for clear and cloudy collocations over sea and non-sea terrains, four (4) corresponding "S " matrices, and nine (9) sets of associated "A" and "N" matrices stratified by latitude and terrain, one set each for clear and cloudy soundings. A total of 28 unique retrieval operators are available, the one used depends upon the latitude, cloud and terrain designation of the satellite sounding.

RESULTS

The following sections illustrate the value of satellite derived products in the analysis of global and regional weather, and is divided into three parts. Part-1 provides a classic illustration of the **information content** of derived sounding products **in the context of NWP** forecasts which assimilate radiance, for a meteorologically active case in the remote, data devoid South Indian Ocean. Part-2 provide a series of **global analysis** illustrating the consistency and meteorological representativeness of (NESDIS) derived sounding products from the current fleet of (three) NOAA operational satellites, followed by a **regional analysis** illustrating consecutive passes of satellite observations and their use in tracking an approaching storm system off the US West Coast. Part-3 provides examples of **vertical statistics** which estimate the accuracy of the satellite derived soundings based on global (ensemble) samples of collocated radiosonde and satellite observations.

Information in the Context of Numerical Weather Prediction (NWP)

The panels in Figure 1 illustrate the information content of the NOAA operational sounding products from ATOVS in the context of NOAA, Environmental Modeling Center (EMC) NWP data (Kalnay *et al.* 1990). The upper two panels show difference fields for **SAT**ellite (NOAA-16) operational soundings minus **NWP** [1] for the 500mb to 300mb layer mean virtual temperature, with the SAT-NWP time differences constrained to be within 2 hours. The middle two panels display analyzed EMC 400mb wind fields (m/s) corresponding to the two upper panels, and the lower two panels are the corresponding AMSU-A channel 5 radiance temperature measurements (K), which are sensitive to middle tropospheric temperature. The region is the remote South Indian Ocean (see EMC panels for latitude and longitude boundaries), on March 23, 2002 (left) and 48 hours later on March 25 (right).

As can be seen, there is a very high correlation among the SAT-NWP difference patterns, the location of the 400mb maximum wind (jet-stream) in the EMC analyzed wind fields, and the satellite measurement data in denoting the frontal zone. This correlation and its persistence over time illustrates the additional information content that derived soundings provide in the context of NWP forecasts, information which may be compromised in current NWP systems which assimilate radiance based on a NWP first guess (McNally et.al., 2000). Unlike NWP which tends to become less reliable in remote frontal zones, the reliability of the derived satellite soundings is not affected by remoteness or ambient weather[2].

---

[1] Available 6 and 12-hour forecasts from the operational Aviation cycle.

[2] The relatively sharp and dynamic nature of the atmospheric structures in frontal zones can enhance the sensitivity of derived products.

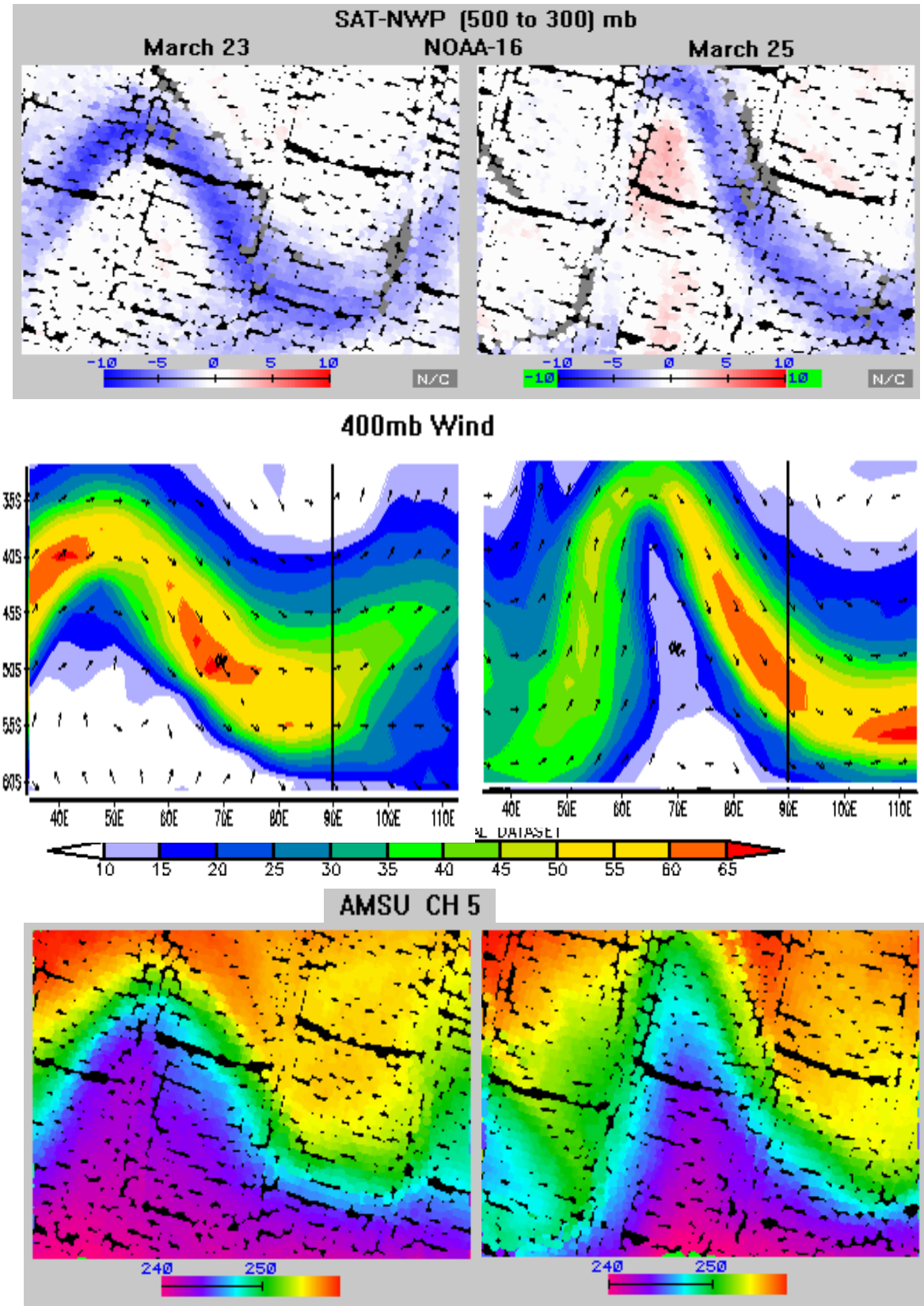

Figure 1: **(SAT-NWP) differences (K) for the 500 to 300mb layer (upper), NOAA/NWP Wind (m/s) Analysis at 400mb (middle), and AMSU-A channel 5 (K) data (lower) over the Indian Ocean on March 23, 2002 (left) and 48 hours later on March 25 (right).**

Patterns such as those shown in Figure 1are not isolated occurrences, but have been observed on a regular basis since the early 1990's (Reale 1995) in conjunction with the initial experiments with the assimilation of NWP-based "interactive" retrievals (Daniels et.al., 1988), and persist today (Reale, 2001 and 2002) in conjunction with current NWP-based "radiance" assimilation (McNally et.al., 2000). The existence of such patterns warrant further study to better understand their importance as a diagnostic tool, and to assist forecasters in identification and prediction of developing storm systems.

Global (and Regional) Analysis

Figures 2 through 7 show a series of color-enhanced, horizontal fields which display NESDIS operational satellite products. Each figure contains a set of four panels, and each panel a global time-composite of the satellite data for selected parameters and satellites. Each of the panels cover the same 12-hour period [3], consisting of approximately seven orbits displayed in a rectangular-Cartesian projection along with the corresponding color scale and data range. Together, the combined fields illustrate the internal consistency and meteorological representation of NESDIS derived weather products through the atmosphere.

Figure 2 shows **SAT**ellite minus **NWP** differences for the 1000mb to 700mb layer mean virtual temperature. The time difference for the SATellite and NWP data vary over +/- 3 hours, and similar to Figure 1 the 6-hour NWP forecasts used are from the Aviation forecast cycle. Differences are shown (clockwise beginning upper left) for the NOAA operational soundings from NOAA-15, NOAA-16, NOAA-17, and for Defense Meteorological Satellite Program (DMSP) operational soundings (Reale *et al.* 1995) from the F-15 satellite. Similar to Figure 1, the difference patterns tend to trace frontal zones, but in this lower layer positive differences (Red) tend to correlate with warm advection and negative differences (Blue) with cold advection zones; in neutral zones or warm/cold cores differences tend to zero (white) (Reale 1995).

Figure 3 illustrates **SAT**ellite minus **NWP** differences (similar to Figure 2) for the 500mb to 300mb layer mean virtual temperature. Once again, very good consistency is observed among the difference patterns for the four independently operated satellite systems. Compared to Figure 2, the differences for this layer are smaller in magnitude, with noticeably more structure in the southern hemisphere and a more definable cold bias. Since the 500mb to 300mb layer represents one of the most reliable regions of the atmosphere with respect to satellite observations and derived products, the importance of these differences in the context of NWP is enhanced particularly in this remote ocean region. The value and consistency of the signature difference patterns illustrated in Figures 1, 2 and 3 for monitoring NOAA operational weather data systems cannot be overstated.

Figure 4 illustrates global time-composite fields of satellite derived cloud mask data (blue is clear, white is cloudy), clockwise beginning in the upper left, for NOAA-15, NOAA-16, and NOAA-17. The cloud mask is important as it determines whether infrared (HIRS) measurements can be used to generate soundings, and as can be seen the consistency among the three operational satellites is very good. The lower left quadrant shows a concurrent image of the AVHRR infrared measurements for

[3] Each satellite measures a different location of the earth at a given time depending on its local equator crossover time.

channel 4 from NOAA-16. AVHRR data are highly sensitive to clouds which contaminate these data resulting in lower values, and are used along with the HIRS to provide the ATOVS cloud mask (Ferguson and Reale 2000). As can be seen, there is good agreement among the global cloud masks for each satellite, and between the colder, contaminated AVHRR data and cloudy regions for NOAA-16.

Figure 5 illustrates global analysis for the satellite derived 850mb water vapor mixing ratio, clockwise beginning in the upper left, from ATOVS for NOAA-15, AMSU-B for NOAA-17, and ATOVS from NOAA-17 and NOAA-16 respectively. Moisture products from AMSU-B are independently derived using a statistical regression approach (Chalfant *et al.* 1999 and Reale 2001)[4]. In general, good consistency among the global moisture patterns are observed, however, areas of difference particularly compared to the AMSU-B products are seen, for example, over northern Africa, and in moisture laden tropical areas where the AMSU-B products show a dry bias of up to 1.5 g/kg. Given the inherent difficulty of validating global moisture given its relatively high spatial/temporal variability, the degree of consistency among these products is encouraging. The problem of deriving global moisture profiles using satellite observations represents one of the foremost challenges for satellite meteorologists.

Figure 6 illustrates 200mb temperature for (clockwise beginning upper left) NOAA 15, NOAA-16 and NOAA-17, with the lower left panel illustrating the corresponding EMC analysis field valid at 00Z (the center point of the 12 hour satellite time-composites). In general, the global 200mb temperature is one of the most difficult parameters to retrieve as it represents the mean location of the tropopause, a region of the atmosphere where associated temperature lapse rate structures can reduce the sensitivity of the satellite sounders. The excellent agreement among the satellites and against the EMC analysis underscores the reliability of the NESDIS scientific approach to provide consistent data even as the information from the sounder is reduced. This can be attributed to the apriori guess, and also the vertical statistical correlation constraints imposed in the retrieval solution through the first guess error correlation "S" matrix of Equation 2.

Figure 7 illustrates upper stratospheric composite fields of 10mb temperature for the four (4) NESDIS operational satellite product systems. The 10mb level is typically above the highest report levels of most conventional radiosonde observations and NWP forecast models, rendering the satellites as a primary source of contiguous global measurements at such levels. Once again, excellent agreement is observed among the four independent satellite derived product Operations.

Figures 8 and 9 integrate selected horizontal field and vertical profile data in a series of single-orbit observations from each satellite over an approximately 7-hour time period, to track an advancing weather front as it approaches the northwest US coast. Such studies simulate a realistic scenario in which forecasters may utilize the information provided by polar satellites in a real-time environment.

---

[4] NESDIS plans to simultaneously process AMSU-B with HIRS and AMSU-A during the Year 2004, see Section 5.

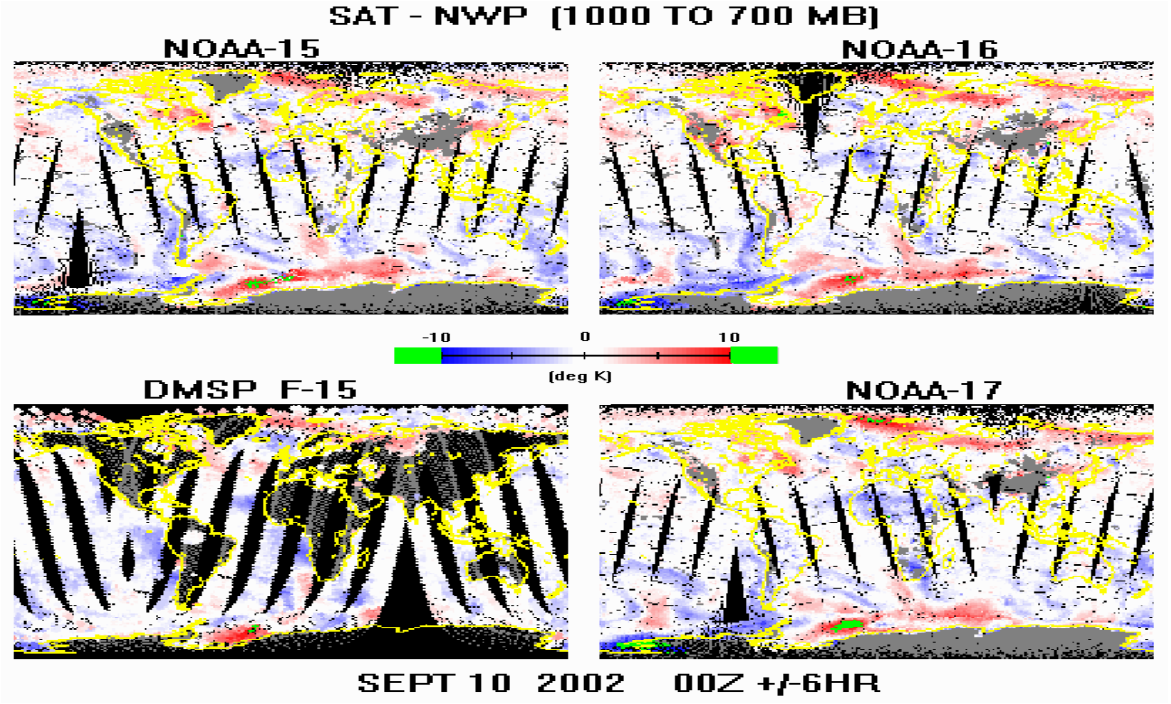

Figure 2: **Satellite sounding minus NWP difference patterns for the 1000mb to 700mb layer mean virtual temperature for the four (4) NESDIS operational sounding systems, composited over the 12 hour period.**

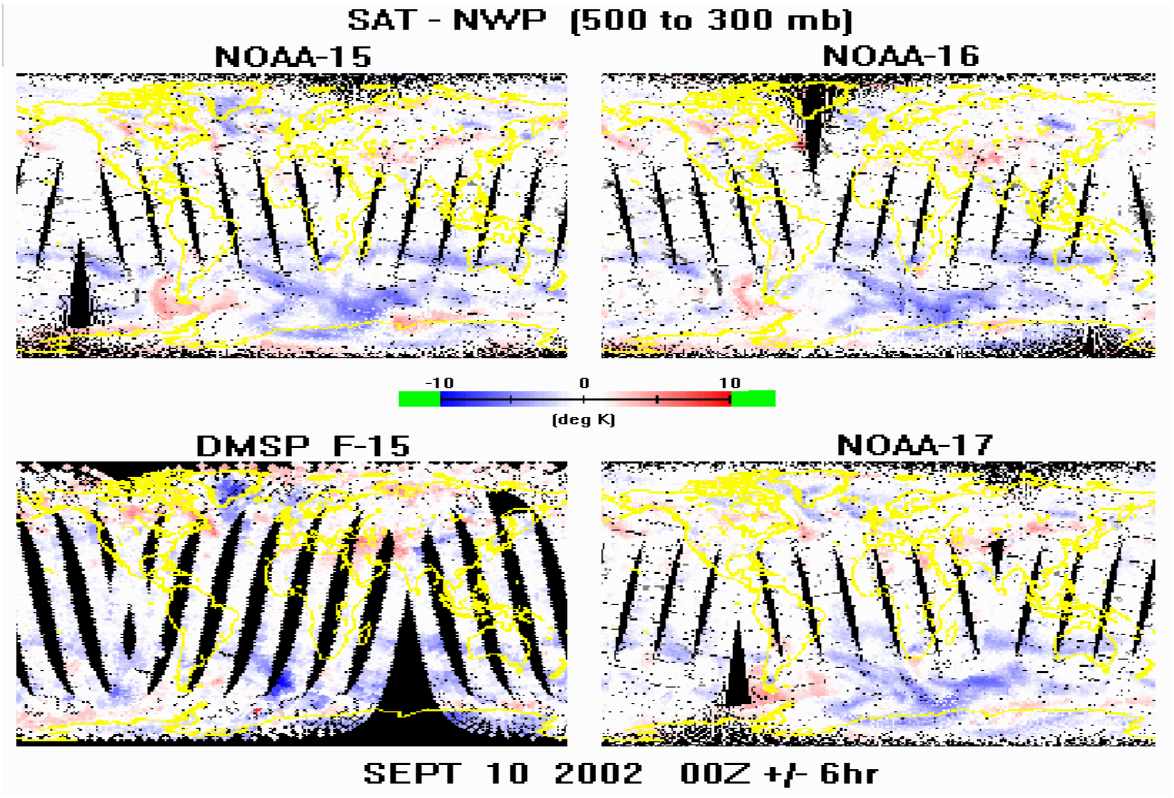

Figure 3: **Satellite sounding minus NWP difference patterns for the 500mb to 300mb layer mean virtual temperature for the four (4) NESDIS operational sounding systems, composited over the 12 hour period.**

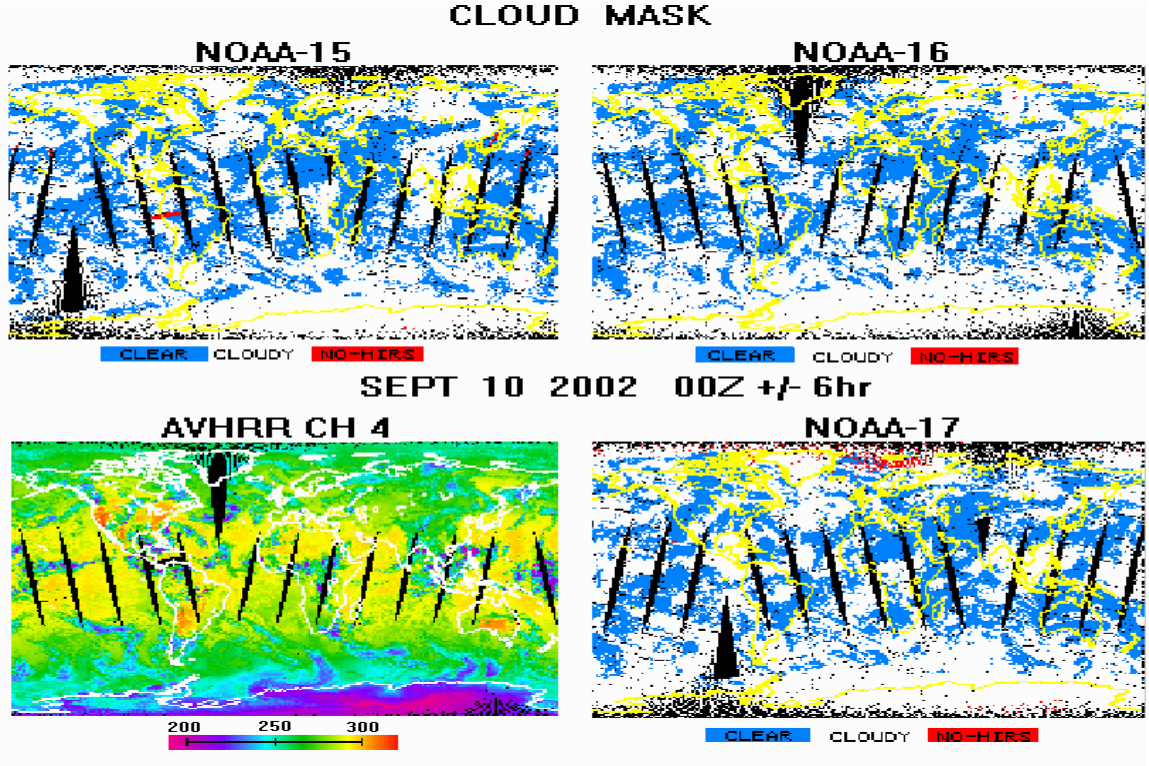

Figure 4: **Satellite derived cloud mask for NOAA-15, 16 and 17 and the corresponding AVHRR channel 4 observations from NOAA-16, composited over the 12 hour period.**

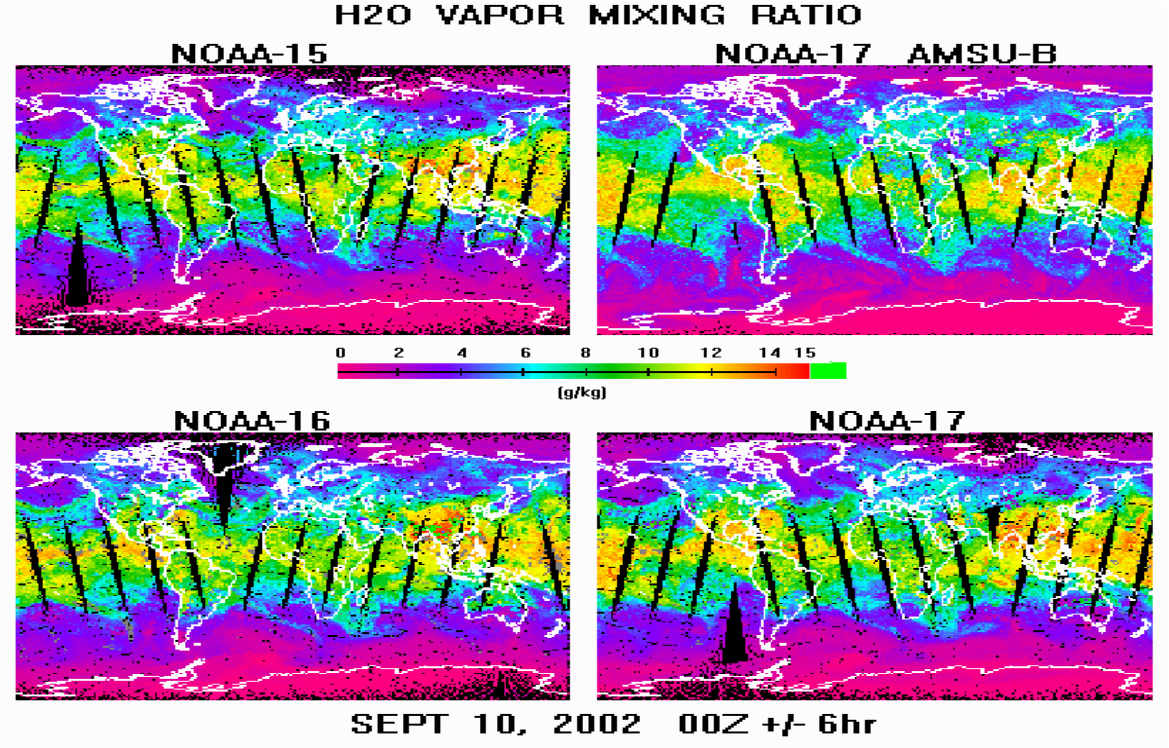

Figure 5: **Satellite derived water vapor mixing ratio (g/kg) for ATOVS from NOAA-15 (upper left), NOAA-17 (lower right) and NOAA-16 (lower left), and for NOAA-17 using AMSU-B only (upper right), composited over the 12 hour period.**

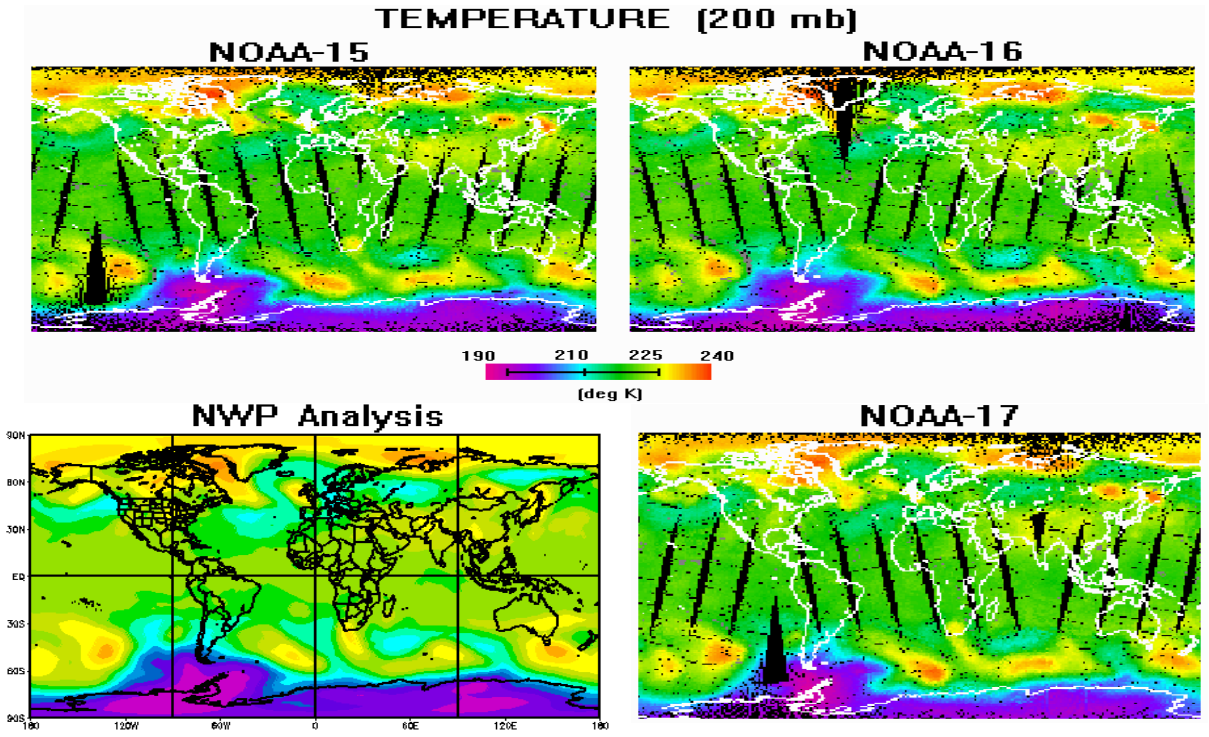

Figure 6: **Satellite derived 200mb temperature (K) from NOAA-15 (upper left), NOAA-16 (upper right) and NOAA-17 (lower right), each composited over the 12 hour period from 18Z Sept.9 thru 6Z Sept. 10, and for the corresponding EMC-NWP Analysis (lower left) valid at 00Z on September 10, 2002.**

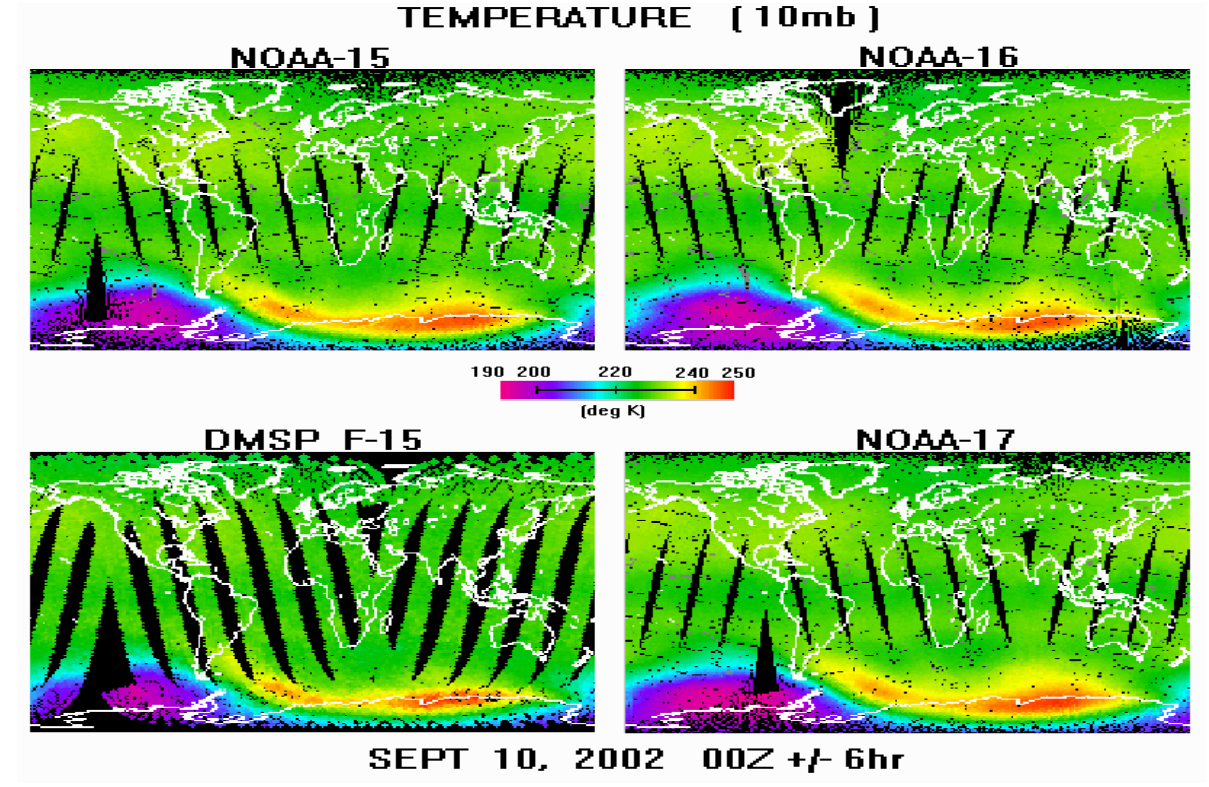

Figure 7: **Satellite derived temperatures at 10mb for the four (4) NESDIS operational sounding systems, composited over the 12 hour period.**

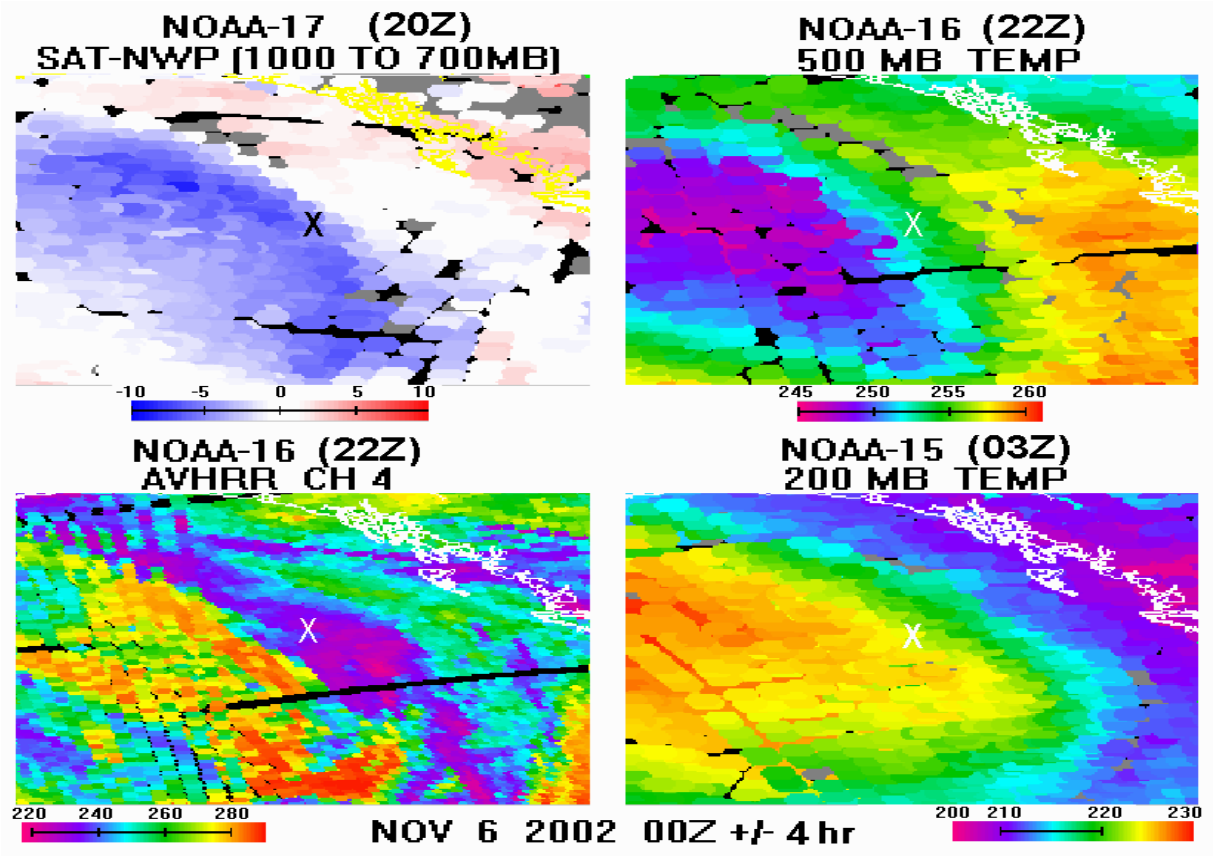

Figure 8: **NOAA-17 satellite minus NWP temperature difference patterns for the 1000mb to 700mb layer (upper left), NOAA-16 retrieved temperature at 500mb (upper right), NOAA-16 AVHRR measurements for channel 4 (lower left), and NOAA-15 retrieved temperatures at 200mb (lower right) for successive passes over a 7-hour period in conjunction with an advancing weather front off the northwest US coast.**

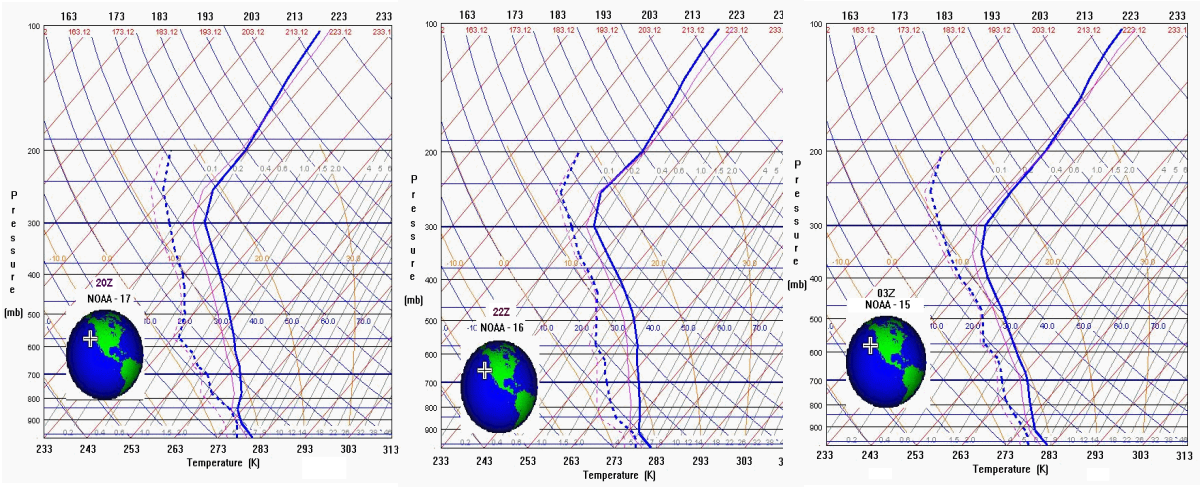

Figure 9: **Satellite sounding temperature (solid) and moisture (dashed) profiles for consecutive passes of NOAA-17 (top) at 20Z, NOAA-16 (middle) at 22Z, and NOAA-15 at 03Z at the location "X" in Figure 8; the associated red curves indicate first guess profiles.**

The two upper panels of Figure 8 illustrate horizontal fields from consecutive passes of NOAA-17(left) and NOAA-16 (right) at approximately 20Z and 22Z, respectively. The NOAA-17 data are the **SAT**ellite minus EMC 6-hour **NWP** differences for the 1000mb to 700mb layer (similar to Figure 2) , and the NOAA-16 data are for 500mb temperature. The two lower panels show corresponding AVHRR data for NOAA-16 (at 22Z) indicating clouds, and 200mb temperature fields from NOAA-15 at approximately 03Z the following day.

The three vertical profiles illustrated in Figure 9 correspond to derived temperature and moisture sounding from the consecutive passes (left to right) of NOAA-17 (20Z), NOAA-16 (22Z), and NOAA-15 (03Z), at the location of the"X"indicated in each of the panels of Figure 8.

The combination of data shown in Figures 8 and 9 show how satellite derived products can assist forecasters in making forecasts particularly in data sparse regions. For example, the panels of Figure 8 show a sharp demarcation of relatively small and decidedly negative differences between the **SAT**ellite data for NOAA-17 and the **NWP,** which line up slightly to the west of the advancing cold front boundary as indicated two hours later in the 500mb temperature and cloud analysis fields from NOAA-16. Some 5 hours later, the 200mb temperature fields from NOAA-15 clearly indicate the sharp stratospheric infusion (lowering tropopause) indicative of subsiding air directly behind the front as it continues to intensify and approach the coast.

The analysis of the series of vertical temperature profiles for each satellite over the seven hour period as shown in Figure 9 is a little more subtle. At first glance there appears to be little difference in the respective profiles, but closer inspection reveals characteristics consistent with cold air advection behind the front, for example, middle tropospheric cooling and the lowering tropopause (stratospheric infusion) height in the latest (03Z) temperature profile from NOAA-15.

Vertical Statistics

The final evaluation strategy concerning satellite derived sounding products are the vertical accuracy statistics based on collocated radiosonde and satellite sounding differences. Such statistics are useful as an overall indicator, but are limited given the spatial and temporal windows for making collocations, subsequent bias in the global sampling bias per satellite (see Part 2), and radiosonde report uncertainties.

Figure 10 provides estimates of the vertical accuracy of the ATOVS temperature soundings for the NOAA-17, 16 and 15. Mean and standard deviation differences are shown for the first guess (light) and final sounding (dark) profiles, with pressure along the x-axis and sample size on the right. The time period is a 7-day period during September, 2002, for combined clear and cloudy soundings from the 60N to 60S latitude belt. As can be seen, mean bias and standard deviation values for the final soundings are typically close to zero and 2.0K respectively, with maximum values near the surface and tropopause, and minimum values in the middle troposphere. Differences for the final soundings are less than those for the first guess throughout the profile for all three satellites, indicating the consistent convergent nature of the final retrieval solution relative to the guess.

Figure 11 show similar statistics but for the ATOVS moisture soundings, showing results (from left to right) for ATOVS from NOAA-17, ATOVS for NOAA-16), AMSU-B for NOAA-17 (Chalfant et.al., 1999), and ATOVS for NOAA-15.

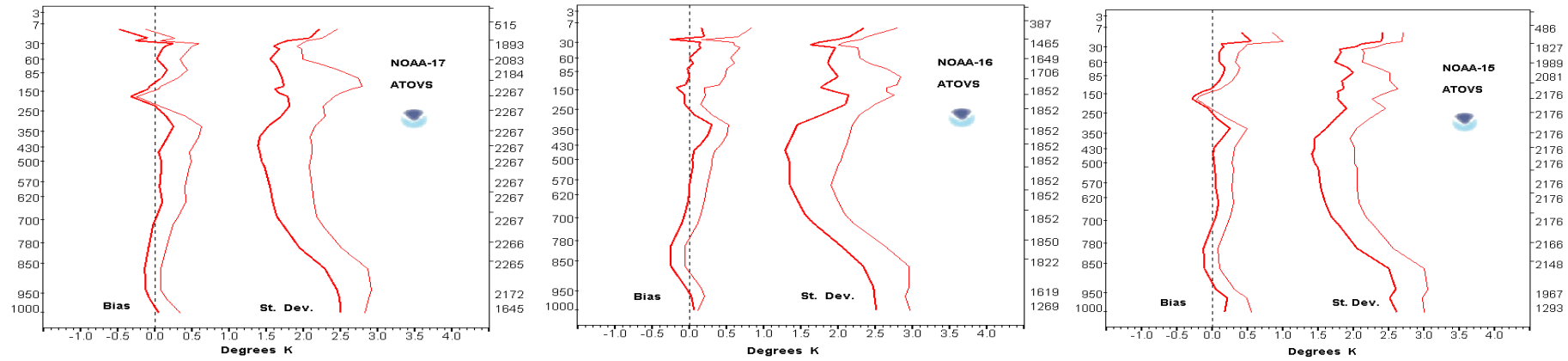

Figure 10: **Vertical statistics of atmospheric temperature (Deg K) differences for derived soundings minus radiosondes from ATOVS NOAA-17 (left), NOAA-16 (middle) and NOAA-15 (right) from the 60N to 60S for the period Sept 2-8, 2002; the atmospheric pressure (mb) and sample size per level are shown along the left and right axis, with heavy curves showing final derived sounding and lighter curves the first guess differences from radiosondes, respectively.**

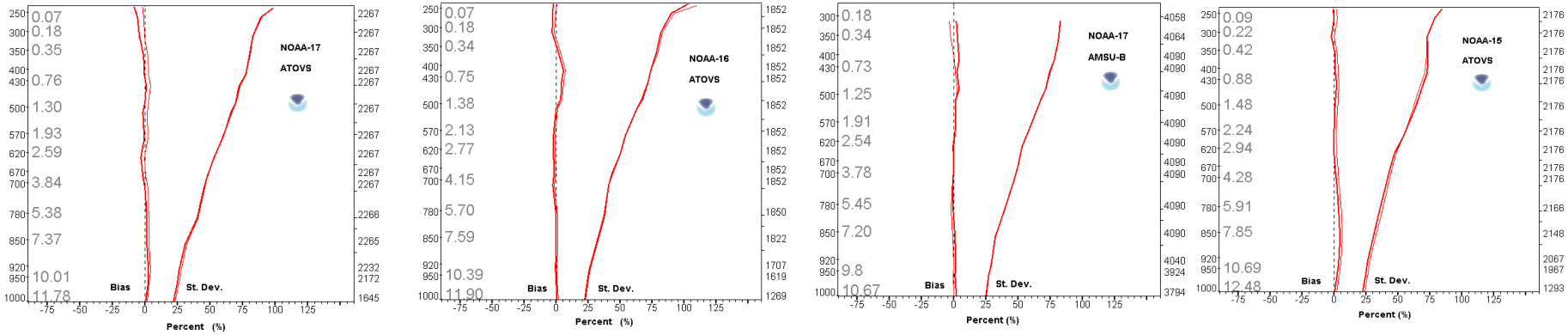

Figure 11: **Satellite minus radiosonde differences in percent (%) water vapor mixing ratio (g/kg) for (left to right) ATOVS from NOAA-17, ATOVS from NOAA-16, AMSU-B from NOAA-17, and ATOVS from NOAA-15, covering the 60N to 60S region over the period Sept 2-7, 2002; the atmospheric pressure and sample size per level are shown along the outside of each vertical axis, with the mean mixing ratio values used to compute percentages inside each left axis.**

The moisture curves represent difference in percent (%) of satellite minus radiosonde moisture at each level based on the mean moisture profiles indicated on the inside of the leftmost axis of each plot (which explains why the values increase with height). A high degree of consistency is observed among the ATOVS moisture soundings from the three operational satellites, and against the AMSU-B products, with estimated accuracies ranging from about 25% [5] near the surface (about 1.2 g/kg) to about 75% (less than .1 g/kg) aloft.

FUTURE PLANS

A new series of science changes for NESDIS derived sounding products are currently under development for ATOVS. Referred to as System-2004, the motivation for these upgrades is to satisfy the greatest common denominator of the total user need, as well as to provide a benchmark capability which is compatible with planned next generation of NPOESS systems (Aumann *et al.* 2003). System-2004 will provide a dual set of "derived" products, first, a more stable and clearly traceable data set of measurements and products suitable for climate, embedded within and serving as the apriori estimates for the more dynamic and traditional second set of real-time weather products for NWP, but one which is well-behaved with respect to the background error problem, explicitly satisfies the measurements within some known uncertainty interval, and is independent of any particular NWP model.

The **scientific upgrades** planned by NESDIS for ATOVS System 2004 derived sounding products include:

- inclusion of AMSU-B measurements in the simultaneous retrieval of temperature and moisture soundings,
- replacement of the library search technique for computing the first guess with an AMSU based statistical regression approach (Goldberg 1999),
- radiative transfer bias adjustment of sounder measurements, and
- more explicit use of radiative transfer (McMillin *et al.* 1995) model to retrieve soundings.

In addition, **peripheral upgrades** to improve ancillary data and products validation in conjunction with the System-2004 modifications will include:

- more stabilized limb adjustment procedures,
- convergence with techniques resident in the NESDIS operational Microwave Surface and Precipitation Products System,
- expanded validation to compare collocated satellite, NWP, and radiosonde data including observed versus calculated radiances, and
- grid satellite parameters.

These upgrades are targeted for a phased operational implementation beginning the Summer of 2004.

---

[5] Values are inflated given the inherent uncertainty in radiosonde moisture measurements and the high spatial and temporal variability of moisture (compared to temperature).

REFERENCES

Allegrino, A., A.L. Reale, M.W. Chalfant and D.Q.Wark, 1999: Application of limb adjustment techniques for polar orbiting sounding data. *Technical Proceedings of the 10th International TOVS Study Conference*, Jan 26- Feb 2, Boulder, Colorado, USA., 1-10.

Aumann, H.H., M.T. Chahine, C. Gautier, M.D. Goldberg, E. Kalnay, L.M. McMillin, H. Revercomb, P.W. Rosencranz, W.L. Smith, D.H. Staelin, L.L. Strow, and J. Susskind, 2003: AIRS/AMSU/HSB on the AQUA mission: design, science objectives, data product, and processing systems. *IEEE Trans. Geosci. Remote Sensing*, Vol 41, pp253-264.

Chalfant, M.W., A. Reale and F. Tilley, 1999: Status of NOAA advanced microwave sounding unit-B products. *Technical Proceedings of the 10th International TOVS Study Conference*, Jan 26-Feb 2, Boulder Co., USA, pp. 60-71.

Daniels, J.M., M.D. Goldberg, H.E. Fleming, B. Katz, W.E. Baker, and D.G. Deaven, 1988: A satellite retrieval/forecast model interactive assimilation system. *12th Conference on Weather Analysis and Forecasting*, AMS, Monterey, Ca..

Ferguson, M.P., and A.L. Reale, 2000: Cloud detection techniques in NESDIS Advanced-TOVS sounding products systems. *10th Conf. on Satellite Meteorology and Oceanography*, 9-14 January, Long Beach, CA

Fleming, H.E., D.S. Crosby, and A.C. Neuendorffer, 1986: Correction of satellite temperature retrieval errors due to errors in atmospheric transmittances. *Journal of Climate and Applied Meteorology*, Vol 25, No. 6, 869-882.

Goldberg, M, J. Daniels and H. Fleming, 1988: A method for obtaining an improved initial approximation for the temperature/moisture retrieval problem. *Preprints, 3rd Conference on satellite Meteorology and Oceanography*, Anaheim, Ca, 16-19.

Kalnay, E., M. Kanamitsu, and W.E. Baker, 1990: Global numerical weather prediction at the National Meteorological Center. *Bull. Amer. Meteor. Soc.*, Vol 71, pp. 1410-1428.

McMillin, L.M., L. Crone and T.J. Kleespies, 1995: Atmospheric transmittances of an absorbing gas. 5. Improvements to the OPTRAN approach. *J. Appl. Opt.*, 34, 8396-8399.

McNally, A.P., J.C. Derber, W.S. Wu, and B.B. Katz, 2000: The use of TOVS level-1B radiances in the NCEP SSI analysis system. *Q.J.R. Meteorol Soc.*, Vol 126, pp. 689-724.

Reale, A.L., 2001: NOAA operational sounding products from advanced-TOVS polar orbiting environmental satellites. *NOAA Technical Report NESDIS 102*, U.S. Dept. of Commerce, Washington D.C., 61 pp.

Reale, A.L., 2002: NOAA operational sounding products for advanced-TOVS: 2002. *NOAA Technical Report NESDIS 107*, U.S. Dept. of Commerce, Washington D.C., 29 pp.

Reale, A.L. 1995: Departures between derived satellite soundings and numerical weather forecasts: present and future. *Tech. proceeding of the 8th International TOVS Study Conf.*, Queenstown, New Zealand, 395-404.

Tilley, F.H., M.E. Pettey, M.P. Ferguson, and A.L. Reale, 2000: Use of radiosondes in NESDIS advanced-TOVS (ATOVS) sounding products. *10th Conference on Satellite Meteorology and Oceanography*, 9-14 January, Long Beach, CA.